Cerebral Cortex Advance Access published June 20, 2011

Cerebral Cortex
doi:10.1093/cercor/bhr146

Unconscious Priming Instructions Modulate Activity in Default and Executive Networks of the Human Brain

Nicola De Pisapia[1], Massimo Turatto[1,2], Pan Lin[1], Jorge Jovicich[1,2] and Alfonso Caramazza[1,3]

[1]CIMeC—Center for Mind/Brain Sciences, University of Trento, Rovereto (TN) 38068, Italy, [2]Department of Cognitive Science and Education, University of Trento, Rovereto (TN) 38068, Italy and [3]Cognitive Neuropsychology Laboratory, Department of Psychology, Harvard University, Cambridge, MA 02138, USA

Address correspondence to Nicola De Pisapia, CIMeC—Center for Mind/Brain Sciences, University of Trento, Rovereto (TN) 38068, Italy. Email: nicola.depisapia@unitn.it.

During task executions, brain activity increases in executive networks (ENs) and decreases in default-mode networks (DMNs). Here, we examined whether these large-scale network dynamics can be influenced by unconscious cognitive information processing. Volunteers saw instructions (cues) to respond either ipsilaterally or contralaterally to a subsequent lateralized target. Unbeknownst to them, each cue was preceded by a masked stimulus (prime), which could be identical (congruent), or opposite (incongruent) to the cue, or neutral (not an instruction). Behaviorally, incongruent primes interfered with performance, even though they were not consciously perceived. With functional magnetic resonance imaging, we individuated the anticorrelated ENs and DMNs involved during task execution. With effective connectivity analyses, we found that DMNs caused activity in ENs throughout the task. Unconscious interference during incongruent trials was associated with a specific activity increase in ENs and an activity drop in DMNs. Intersubject efficiency in performance during incongruent trials was correlated with functional connectivity between specific ENs and DMNs. These results indicate that unconscious instructions can prime activity in ENs and DMNs and suggest that the DMNs play a key role in unconscious monitoring of the environment in the service of efficient resource allocation for task execution.

Keywords: attention, awareness, brain networks, executive functions, masking

Introduction

Neuroimaging research has typically assumed that cognition can be studied by looking at activity in isolated brain regions, but in recent years, the perspective is gradually shifting toward the view that cognitive functions should also be studied as resulting from large-scale network interactions (Bressler and Menon 2010). Thus, when humans perform stimulus-based tasks, it has been consistently found that activity increases in the executive network (EN) and decreases in the default-mode network (DMN) (Fox et al. 2005; Fox, Corbetta, et al. 2006; Golland et al. 2007; Lin et al. 2011). EN components include a "central" part (dorsolateral prefrontal and superior parietal areas) and a "salience" part (ventrolateral prefrontal, anterior cingulate, and anterior insular cortex) (Seeley et al. 2007; Sridharan et al. 2008; Kim 2010), whereas DMN components—which are consistently more active during rest and defocused internal thinking (mind wandering)—include medial prefrontal, posterior cingulate, hippocampus, superior temporal, and inferior parietal regions (Raichle et al. 2001; Greicius et al. 2003; Damoiseaux et al. 2006; Fox, Corbetta, et al. 2006; Fransson 2006; Buckner et al. 2008; Christoff et al. 2009; Andrews-Hanna et al. 2010). DMN deactivations during task executions have been interpreted as allowing efficient resource allocation in favor of EN (Weissman et al. 2006). Several studies support the view that behavioral performance in externally oriented tasks is strictly linked to intrinsic activity in DMN (Fox, Snyder, et al. 2006; Mennes et al. 2011) and to DMN's functional connectivity with EN (Kelly et al. 2008; Mennes et al. 2010). Recent studies also suggest that DMN components monitor and cause activity in EN (Uddin et al. 2009). Thus, the emerging view is that DMN activity—far from being only rest related—is an essential portion of task-related processing.

In the present study, we investigated whether these task-related network dynamics can be modulated by unconscious information. There is much evidence showing that unconscious stimuli, mostly hidden to awareness through visual masking techniques (Breitmeyer 2007), can nonetheless modulate brain activity in visual and semantic brain regions (Kouider and Dehaene 2007). A few recent studies (Lau and Passingham 2007; van Gaal et al. 2008; van Gaal et al. 2010) have additionally shown that masked instructions can influence operations and activity in specific executive regions. In Lau and Passingham (2007), participants were cued to make either a semantic or a phonological judgment to a word stimulus, but masked instructions primed them to perform either the same or the alternative judgment. They investigated activity in specific lateral prefrontal regions, known to be more active during the execution of those types of judgments, and they found sensitivity to the congruency of the visible and the unconscious instructions. Similarly, in van Gaal et al. (2008, 2010), they found that unconscious NO-GO signals slowed down GO responses or even triggered full response inhibition, influencing activations in inferior prefrontal cortex, an area known to increase its activity during inhibition of responses. These results are particularly interesting because of their implications for the debate concerning the extent to which executive functions should be exclusively associated with consciousness and free will (Dehaene and Naccache 2001; Jack and Shallice 2001; Rees et al. 2002; Hommel 2007; Haggard 2008), and they suggest that unconscious information can trigger and influence executive control.

In the present study, we extend this research on the effects of unconscious priming of instructions by evaluating their impact not just on specific executive regions of interest (ROIs) but on large-scale ENs and DMNs. Volunteers were shown instructions (cues) to respond either ipsilaterally or contralaterally to a subsequent lateralized target. Unbeknownst to

them, each cue was preceded by a masked stimulus (prime), which could be congruent with the cue (i.e., the same instruction), incongruent with the cue (i.e., the opposite instruction), or neutral (i.e., not an instruction). We identified the brain networks involved during task execution, their functional and effective connectivity, their sensitivity to the unconscious primes, and how connectivity correlated with performance. Given the previously mentioned studies on unconscious effects in executive regions, we expected to find that masked primes modulate activity in EN components, but our main goal was to investigate the effects on intrinsic activity in DMN.

This interest in DMN was justified by several lines of evidence indicating that information processing and activity regulation in this network might take place also in the absence of awareness. One line of evidence comes from studies interpreting DMN activity as mainly involved in self-oriented processing, internal mentation, and mind wandering. It is known that mind wandering can take place without participants' awareness and against their intentions, with the effect that it interferes with consciously executed externally oriented tasks (Christoff et al. 2004, 2009; Smallwood and Schooler 2006; McVay and Kane 2010). An alternative function attributed to DMN (Buckner et al. 2008) is of acting as a continuous and passive gatherer of information about the external world in an unfocused manner, working in the background like a radar or a sentinel. DMN activity has been shown to take place without active conscious effort, with the automatic capacity to monitor the environment (Shulman et al. 1997; Gusnard and Raichle 2001; Gilbert et al. 2007; Hahn et al. 2007). Other evidence indicating that coherent activations in this functional network can work independently of consciousness comes from the finding that DMN is active even during unconscious states, such as the descent to sleep (Larson-Prior et al. 2009), light sedation (Greicius et al. 2008), or deep anesthesia in humans (Martuzzi et al. 2010) and also in monkeys (Vincent et al. 2007). DMN has also been found to be tonically active in volunteers performing an implicit memory task but not when explicit retrieval was required (Yang et al. 2010). Finally, in a study of free motor decisions (pressing a left or a right button), it was found that activation patterns in medial prefrontal and posterior cingulate cortex predicted motor decisions up to 10 s before subjects were conscious of them (Soon et al. 2008). These 2 regions are key medial components of the DMN, thus suggesting that this network might play a central role in the unconscious processing of decision-making information. Given all these indications, in the present study, we directly tested the hypothesis that DMN processes unconscious task-related information in a visual masking design.

A crucial property of our study is that the unconscious stimuli consisted of instructions on how to respond (ipsilaterally or contralaterally), but the actual response (to press the left or right response key) depended on where the target subsequently appeared on the screen. In this way, the unconscious stimuli were not priming specific motor responses but response instructions. In other words, based on the mere exposure to these unconscious instructions, participants could not anticipate the required response, but they had to wait until exposure to the specific target before a motor response could be specified. Therefore, priming effects in this design could not be explained in motor terms because no specific motor response was primed. The choice of this experimental design, also adopted in Lau and Passingham (2007), was to specifically activate regions involved in executive control and not in motor planning.

Another crucial aspect of our study is that, in addition to congruent and incongruent unconscious primes, we also used unconscious neutral stimuli, to which no instruction was attached. This choice was made to clarify 2 important points. First, this allowed us to determine whether any observed priming effects were due to of facilitation or interference (Leonard and Chiu 2007). Second, this allowed us to investigate whether any unconscious priming effects were purely visual or linked to executive control. This could be done because in the neutral condition the difference between the prime and the cue was only visual, whereas in the incongruent case it was also in the preparation to execute either an ipsilateral or a contralateral response. Thus, a comparison between brain activities in incongruent versus neutral trials could reveal changes specifically linked to unconscious priming in task-set preparation and not in visual perception.

Another issue addressed here concerns whether the degree of control effort required for the execution of a task determines the extent to which unconscious instruction primes can affect performance. In our task, the instructions required ipsilateral or contralateral responses, but the first are known to involve less control than the second, due to a spatial stimulus–response compatibility effect (Proctor and Reeve 1990). And, in fact, ipsilateral responses are invariabily found to be faster and more accurate than contralateral responses. In addition, in order to make sure that contralateral responses required more control than ipsilateral responses, each block of our experiment included a higher percentage of ipsilateral (75%) than contralateral (25%) responses. Such regulation of overall control at the block level has been adopted in several other studies on executive control (West and Baylis 1998; Kane and Engle 2003; De Pisapia and Braver 2006), so as to induce in participants a higher expectation for one type of trial versus another. With this manipulation, we could therefore test if the differential degree of control effort required by the 2 unconscious instructions determined comparable priming effects.

Our procedure and analyses consisted of several steps in succession. First, we looked for priming effects at the behavioral level, as an obvious precondition before we could proceed to investigate brain activity. We then used functional magnetic resonance imaging (fMRI) during the execution of this task, and we looked for a replication of the priming effects in the scanner. We then analyzed brain activity with group Independent Component Analysis (ICA), a widely used data-driven method to individuate and separate temporally coherent networks based on all voxels. We then used time-course activities of the individuated networks to investigate their functional and causal relationship during task execution. The general linear model (GLM) was used to characterize activation differences during the various prime/cue combinations in regions belonging to the individuated networks. As a last step, we assessed the impact of the unconscious primes with an analysis of how individual differences in performance correlated with the functional connectivity between ENs and DMNs. In this analysis, we expected to find that the anticorrelations between default and executive components would be stronger in subjects performing less efficiently, particularly in the more demanding conditions, as found in Kelly et al. (2008).

Materials and Methods

Forty-six right-handed participants took part in this study (27 females, mean age = 24.8 years, age range 19–43 years). Of these, 26 volunteers (17 females) took part in a behavioral-only experiment (no scanning) and 20 volunteers (10 females) took part in a functional neuroimaging experiment that included both behavioral and scanning components. For one of the volunteers in the neuroimaging experiment, we could not collect reaction times (RTs) due to a technical problem with the button box. No participant had a history of psychiatric illness or neurological disease. They gave written informed consent to participate in this study, according to guidelines set by the Ethical Committee of the University of Trento.

Behavioral-Only Experiment and Analysis

The behavioral-only experiment was divided into 2 parts (see Fig. 1, which also includes exact stimuli durations). First part—participants had their left and right indexes, respectively, on a left and right button. Half of them were instructed that—on each trial—if they saw a small central square (cue), they had to quickly respond on the same side of a subsequently flashed and lateralized target (a circle); if they instead saw a small central diamond, they had to quickly respond on the opposite side of the target (visual angle of all shapes was 1.5°). For balancing, the other half of participants were instructed with the reverse stimulus-to-rule mapping (diamond for ipsilateral and square for contralateral). Unbeknownst to them, each explicit instruction was preceded by a masked prime ("backward metacontrast masking" [Breitmeyer and Öğmen 2006]), which could be an instruction congruent or incongruent with the cue (small square or diamond) or neutral (star) (visual angle 1°). Targets were presented to the left or to the right of the central cue and also above or below the level of the central cue, so as to make their appearance more unpredictable; cues and primes were always presented centrally. After a short practice session with both kinds of trials (14 trials), participants started the experiment proper, consisting of 2 blocks (75% ipsilateral cues, 25% contralateral cues, each block with 144 trials). Second part—after the first part, we informed participants of the presence of the masked stimuli, we showed a slow motion video of a trial, and we asked them to identify the primes in a block of 72 trials (visual design identical to the first part). Their responses consisted in pressing 3 different buttons (one for each shape), and they were asked to respond at their leisure.

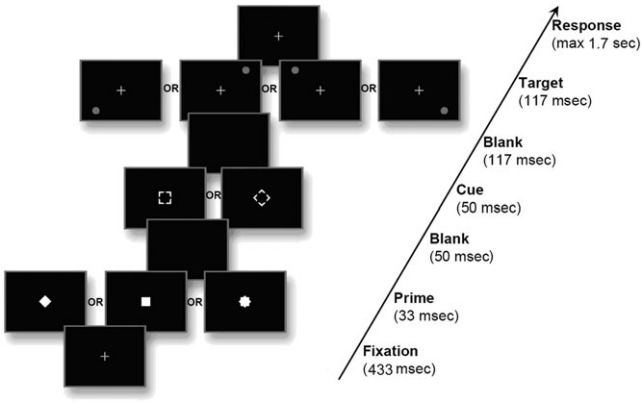

Figure 1. Experimental design. The experiment consisted of 2 parts with an identical sequence of stimuli. Part 1—participants first saw an instruction (cue) to make either an ipsilateral or a contralateral button press (respectively, coded square and diamond for half participants and the inverse for the other half); then they saw a lateralized target (circle), to which they had to quickly respond according to the instruction for that trial (left and right indexes, respectively, on a left and right button). Unbeknownst to them, each explicit instruction was primed by a masked instruction (prime; small square, diamond, or star), which could be congruent (i.e., the same shape) or incongruent (i.e., opposite shapes) with the mask or neutral (star). After a short practice (14 trials), participants started the proper experiment with blocks including 75% ipsilateral cues and 25% contralateral cues (144 trials). Part 2—participants were informed about the presence of masked stimuli and asked to recognize them in a visual design identical to part 1. They could press 3 different buttons (one for each shape) and they responded at their leisure.

Stimuli in both parts of the experiment were presented using ASF ("A Simple Framework," available from jens.schwarzbach@unitn.it), based on the MATLAB Psychtoolbox-3, (Brainard 1997). Behavioral performance data were analyzed via analyses of variance (ANOVAs) or paired *t*-tests on the RT measures and accuracy.

Neuroimaging Experiment

A different group of participants underwent fMRI scanning while performing a task very similar to the one used in the behavioral-only experiment (including the stimulus-to-rule balancing), with only the following differences. Each run of the first part consisted of 3 fixation blocks lasting 16 s each (beginning, middle, and end) and 2 intermixed task blocks (identical to the behavioral only), each lasting 300 s (96 trials in total for each run, 75% ipsilateral and 25% contralateral, with the 3 balanced unconscious primes, as for behavioral-only participants). A random variable interval of 2000 ms (50% of trials), 3000 ms (33%), or 6000 ms (17%) occurred between trials (jittering) to better estimate the event-related hemodynamic response on each trial. Stimuli were presented with a LCD projector (model 150) on a screen positioned at the head end of the bore. Participants viewed the screen through a mirror attached to the head coil. A button box was used to record participants' behavioral performance (left and right indexes on separate MRI-safe pads). After the scanning session, subjects participated in the prime identification part of the experiment while still in the scanner.

For technical reasons, we could not record RTs of button presses during the 2 runs of the first subject (but we could record which button was pressed and check that he performed the task correctly). Stimuli were presented using ASF as for the behavioral-only part.

Image Acquisition

Imaging data were acquired using a 4-T Bruker MedSpec Biospin MR scanner and a birdcage transmit, 8-channel receive head radio frequency coil. Functional images were acquired with a single-shot T_2^*-weighted gradient-recalled echo-planar imaging (EPI) sequence. We used 34 slices, acquired in ascending interleaved order, slightly tilted to run parallel to the calcarine sulcus, with a time to repeat (TR) of 2500 ms (voxel resolution, 3 × 3 × 3 mm^3; time to echo [TE], 33 ms; flip angle [FA], 73°; field of view [FOV], 192 × 192 mm^2; slice gap, 0.45 mm). Each run consisted of 210 volumes. To correct for distortions in geometry and intensity in the EPI images, we applied distortion correction on the basis of the point-spread function data acquired before the EPI scans (Zaitsev et al. 2004). There were 2 dummy scans, and before further analysis, we discarded 2 further volumes. To be able to coregister the low-resolution functional images to a high-resolution anatomical scan, we acquired a T_1-weighted anatomical scan (magnetization prepared rapid gradient echo; 1 × 1 × 1 mm^3; FOV, 256 × 224 mm^2; 176 slices; GRAPPA acquisition with an acceleration factor of 2; TR, 2700 ms; TE, 4.18 ms; inversion time, 1020 ms; 7° FA).

Independent Component Analysis

After discarding the first 2 scans, fMRI data (all subjects and all runs) were processed using the SPM8 software (Wellcome Department of Cognitive Neurology, London, UK; http://www.fil.ion.ucl.ac.uk/spm/). Preprocessing consisted in motion correction, spatial smoothing (4-mm full-width at half-maximum Gaussian kernel), high-pass filter, and normalization of the functional images to the MNI152 standard brain space through their structure images. The preprocessed fMRI data set was analyzed using the Infomax ICA Algorithm available in the Group ICA of fMRI Toolbox (GIFT, http://icatb.sourceforge.net/groupica.htm). The number of estimated components was set to 20, to trade-off between preserving the variance while individuating actual network components and not isolated regions. Group spatial ICA was obtained by concatenating data from all subjects and then reducing this aggregated data set to 20 temporal dimensions using principal component analysis and then an ICA estimation using the Infomax ICA algorithm (Bell and Sejnowski 1995). Individual time courses and spatial maps were then back reconstructed using the aggregated

components and the results from the reduction. Time courses correspond to the waveform of patterns of coherent brain activities across all the voxels and then represented in spatial maps. The final maps were obtained by converting intensity values to *Z*-values, removing the average, and dividing by the standard deviation of the intensity distribution (Calhoun et al. 2001). Finally, we visually inspected the resulting 20 independent components and removed obvious artifacts from the data (e.g., components linked to ventricles, edges, eye movement, and cardiac-induced pulsatile artifact at the base of the brain) (Kelly et al. 2010), which left us with a final list of 14 networks, which we labeled based on the patterns of activations (see Table 1).

Clustering Analysis

For each subject, we computed pairwise temporal correlations based on the ICA time course of each individuated network. For visualization purposes, the averaged Pearson correlation values were ordered according to how numerically close they were to each other. To this end, we used a *k*-nearest neighbor algorithm, a machine learning classifier in which an object is assigned to the class most common among its *k*-nearest neighbors (software available at http://www.eigenvector.com/MATLAB/corrmap.html). In the resulting map (Fig. 3), the scale gives the mean correlation coefficient for each network pair (coefficients have been normalized, such that the highest correlation $r = 0.59$ was set to 1 and the strongest anticorrelations $r = -0.42$ was set to −1).

Granger Causality Analysis

To assess the causal interactions between ENs and DMNs, we used Granger causality analysis between the ICA time courses. Granger causality analyses (Seth 2005) are used to characterize causal interactions through predictability of blood oxygen level–dependent (BOLD) changes between time-course activity of single voxels or small ROIs (Goebel et al. 2003; Roebroeck et al. 2005) and more recently also between time-course activity of ICA components, which must be intended as an entirely data-drive method to detect relationships between large networks of activated voxels in potentially spatially distant regions (Londei et al. 2007; Jafri et al. 2008; Demirci et al. 2009). To perform this analysis, we adopted the functional network connectivity Toolbox (available at http://www.ece.unm.edu/~vcalhoun/mialab/Software/fncimg.html), an extension of the GIFT toolbox (Jafri et al. 2008; Demirci et al. 2009). The toolbox adopts an individual P level of $P < 0.05$ and a group $P < 0.05$ and then allows assessment of outward and inward causal effects (each ICA time course can both be the cause and the effect of other time courses). Additionally, this toolbox presents the causal relationships over portions of the frequency spectrum, to better differentiate if these are driven by low and or high frequencies in the time-course activities (Cordes et al. 2001; Demirci et al. 2009). Causal relationships were computed separately for each participant to allow random effects analyses and false discovery rate correction for multiple comparisons (q(FDR) < 0.05) (Genovese et al. 2002).

Table 1
List of ICA components, after removal of artifacts (e.g., ventricles and edges)

Component	Cluster	*X*	*Y*	*Z*	BA	Name
DMN 1	1	−2	50	28	9/10	Superior medial prefrontal
	2	−4	−52	37	23	Posterior cingulate/precuneus
	3	47	17	−11	20	Superior temporal gyrus
	4	−49	19	−11	20	Superior temporal gyrus
DMN 2 (TPJ)	1	1	−55	53	7	Precuneus
	2	46	−65	25	39	Temporal–parietal junction
	3	−42	−72	28	39	Temporal–parietal junction
DMN 3 (PCC)	1	−2	−60	29	23	Posterior cingulate cortex
DMN 4 (MPFC)	1	−2	53	7	10	Medial prefrontal
Hippocampus	1	25	−35	7		Hippocampus
	2	−27	−38	7		Hippocampus
Precuneus	1	0	−65	43	7	Precuneus
Central EN	1	46	29	21	45/48	Inferior prefrontal
	2	−48	12	29	44	Middle frontal gyrus
	3	43	11	31	44	Middle frontal gyrus
	4	−34	−65	46	7	Superior parietal
	5	29	−65	43	7	Superior parietal
Salience EN	1	43	43	2	45	Inferior prefrontal
	2	0	20	32	24	Anterior cingulate
	3	−40	17	−6		Anterior insula
	4	40	13	−7		Anterior insula
	5	−62	−34	31	40	Superior marginal gyrus
Left visuo-motor	1	−40	−60	50	7	Superior parietal
	2	−48	18	30	44	Inferior prefrontal
Right visuo-motor	1	42	−56	47	7	Superior parietal
		45	28	31	44	Inferior prefrontal
Auditory	1	58	−4	4	22	Superior temporal
	2	−58	4	4	22	Superior temporal
Visuo-motor	1	52	12	26	44	Inferior prefrontal
	2	−42	−45	53	7/40	Superior parietal
	3	34	−44	57	7/40	Superior parietal
Visual 1 (associative)	1	31	−75	25	19	Middle occipital gyrus
	2	−28	−83	23	19	Middle occipital gyrus
Visual 2	1	0	−74	7	17	Cuneus

Note: Labels for each component were assigned by visual inspection. Labels DMN1 to DMN4 refer to DMN components. For each node present in the network, we report Talairach coordinates (*x*, *y*, *z*) (Talairach and Tournoux 1988), the corresponding Brodmann's area label (BA), as well as the anatomical name. See also Supplementary Figure 1 for visualization of these networks on sections of a normalized brain.

General Linear Model Analysis

To explore functional networks' sensitivity to unconscious primes, we conducted 2 orthogonal types of analyses: 1) whole-brain statistical contrasts in the various conditions (including the 6 prime/cue combinations of correct trials and an extra condition for error trials) and 2) ROI analyses, in which functional ROIs were created by defining a 9 × 9 × 9 mm cube centered on the foci (maxima in the statistical maps) of the default and executive components individuated with the group ICA (Table 1). Both types of imaging data analyses were performed with BrainVoyager QX 2.1 (Brain Innovation). For preprocessing, we performed 3D motion correction with trilinear interpolation and slice timing correction with ascending interleaved order, using the first slice as reference. Functional data were temporally high-pass filtered at 3 cycles/run length. A Gaussian kernel of 4 mm was applied to spatially smooth the images. Next, we aligned the first volume of each functional run to the high-resolution anatomy. Both functional and anatomical data were transformed into Talairach space (Talairach and Tournoux 1988), using trilinear interpolation. Predictor time courses were convolved with a canonical hemodynamic impulse response function starting at the initial fixation for each trial, also including 3D motion correction parameters. For all reported contrasts, we used random effects, and FDR to correct for multiple comparisons (q(FDR) < 0.05) (Genovese et al. 2002).

Interindividual Brain–Behavior Relationship

We analyzed how the strength of the anticorrelations between default and executive components related to performance. As a measure of performance, we used the mean RTs in the various conditions. We computed the correlations between this performance value and the Pearson correlation between default and executive components, separately in ipsilateral and contralateral trials, also dividing in the congruent, neutral, and incongruent cases. Importantly, we also kept the 2 runs of each subject separated, thus we had 2 RT means for each subject. For technical reasons, we could not record RT of the first subject, thus his data were not computed (even though we could register his responses, and thus we could check that he was doing the task correctly, therefore we used his fMRI data).

Results

We first describe the effectiveness of the visual masking procedure. We then report the behavioral results outside and inside the fMRI scanner. We then list the functional brain networks involved in the task, their causal relationships, their specific sensitivity to the unconscious primes, and how intersubject efficiency in performance was a function of anticorrelations between specific default and executive components.

Behavioral Data

Visibility of Unconscious Instructions

In line with previous studies, to keep the primes below conscious accessibility, we used backward metacontrast masking (Breitmeyer and Öğmen 2006). As in other studies on unconscious perception (Sergent et al. 2005; Del Cul et al. 2007), our first criterion of effective masking was to simply ask participants at the end of part 1 if they had noticed the presence of stimuli preceding the cues in any of the trials. Ninety percent of the participants responded that they never saw anything preceding the cues, whereas the remaining 10% reported seeing something odd (like a whitish blob or an expansion), but only in the first few trials of practice, and without clearly identifying what. After we informed all participants about the presence of the masked stimuli and showed them a slow motion video of a trial, none of the subjects reported ever seeing the primes before the cues. In a separate block (part 2), they were asked to focus on the primes and report what they saw by pressing 1 of 3 buttons (relative to square, star, or diamond), which they could press at their leisure. As an additional objective measure of effective masking for all subjects (inside and outside of the scanner), we computed their sensitivity to the prime during this separate block by calculating *d'* (Macmillan and Creelman 1991), which on average for all subjects (both behavioral-only and fMRI volunteers) was 0.07, not significantly different from 0 ($P > 0.3$), with a standard deviation of 0.38.

Task Performance

Mean RTs for all participants—combining those who participated in the behavioral-only and the fMRI experiments—for ipsilateral trials were: congruent RT = 500.7 ms, neutral RT = 505.9 ms, incongruent RT = 538.7 ms. Mean RTs for contralateral trials were: congruent RT = 551.0 ms, neutral RT = 554.0, incongruent RT = 582.0. Thus (see Fig. 2), for both ipsilateral and contralateral trials, there was an interference effect (incongruent RT minus neutral RT) and no facilitation effect (congruent mean RT minus neutral mean RT). To verify these results, we performed a three-way ANOVA (2 × 2 × 3) on mean RTs with the following factors: "group" (behavioral-only or fMRI), "response-type" (ipsilateral or contralateral), and "congruency" (congruent, neutral, and incongruent) between the unconscious prime and the mask (i.e., the visible cue). Main effects of all factors were significant (group $P < 0.001$, response-type $P < 0.001$, prime/cue congruency $P < 0.01$), and there was no interaction (min $P = 0.74$). The main effect of the group factor indicates that there was a significant overall delay (behavioral-only RT = 476.95 ms, fMRI RT = 623.22 ms) induced by the different set-up in the MR scanner (volunteers lying on the scanner bed, looking in a small mirror, and pressing buttons on pads) compared with the behavioral-only set-up (volunteers sitting at a desk, in front of a monitor, and pressing keys on a keyboard), but this did not interact with the other factors. To further qualify the effects of the response-type and congruency factors, we performed paired *t*-tests between the congruent and incongruent conditions versus the neutral conditions (separately for congruent and incongruent trials, to further verify that there was no interaction between the 2 factors) and corrected for multiple comparisons (FDR). RTs of congruent trials resulted not significantly different from RTs of neutral trials ($P = 0.2$ and $P = 0.6$, respectively, for ipsilateral and contralateral trials, corrected), thus showing that there was no facilitation effect due to the presence of the subliminal primes. RTs for incongruent trials were instead different from RTs for neutral trials (ipsilateral $P < 0.001$; contralateral $P < 0.01$, corrected), thus showing that there was a significant interference effect.

Mean error percentages were very low. For ipsilateral trials, they were: congruent = 3.4%, neutral = 4.2%, incongruent = 5.2%; for contralateral trials: congruent = 4.6%, neutral = 5.4%, incongruent = 6.8%. Paired *t*-tests (corrected with FDR) confirmed a significant difference in error percentages only between ipsilateral congruent trials and ipsilateral incongruent trials ($P < 0.05$, corrected).

In sum, the main behavioral result was that performance was worse when unconscious instructions were incongruent with the visible masking instructions. Furthermore, interference took place independently of whether the unconscious prime regarded an easier (ipsilateral) or a more difficult (contralateral) response. This interference appeared to take place at the task-set level and not at the perceptual level because the unconscious neutral instruction—visually different from the subsequent conscious instruction—did not impair performance, either in RTs or in accuracy.

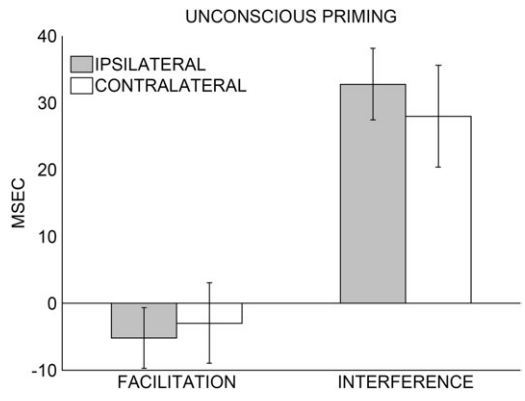

Figure 2. Facilitation (congruent RTs minus neutral RTs) and interference (incongruent RTs minus neutral RTs) effects for all volunteers (behavioral-only and in the fMRI scanner), shown separately for ipsilateral and contralateral trials. There were ipsilateral and contralateral interference effects due to incongruency between the unconscious prime and the visible cue, and no facilitation effect when there was congruency (see also statistical analyses). Error bars are standard errors.

Neuroimaging Data

Independent Component Analysis

ICA of the neuroimaging data allowed us to individuate the coherent brain networks involved during task execution, as opposed to single regions of activity (Esposito et al. 2006; Calhoun et al. 2008). After removal of artifacts (e.g., ventricles and edges), we identified a number of networks, including default and executive components, as reported in Table 1.

Clustering Analysis

To investigate the temporal correlations between the ICA components listed in Table 1, we used clustering analyses of the Pearson correlation between their time courses (Fig. 3). The results confirmed that during the execution of the task, brain activities were split into 2 opposed systems: a group of coherent

networks, which included executive components, and an anticorrelated group including default mode components.

Granger Causality Analysis

To investigate the causal connectivity between the individuated default and executive components, we performed a Granger causality analysis of their ICA time courses (casual connectivity graph is illustrated in Fig. 4). This analysis revealed 4 fundamental relationships (all surviving FDR correction for multiple comparisons): 1) DMN components influence each other (DMN3 [PCC] influenced the components DMN1 and DMN4 [MPFC], and DMN4 [MPFC] influenced DMN2 [TPJ]); 2) DMN3 (PCC) plays a key top-down role not just in DMN (previous point 1) but also relative to salience EN and the visuo-motor coordination components; 3) the salience EN component is influenced by both DMN (DMN1, DMN2 [TPJ] and DMN3 [PCC]) and the visuo-motor coordination component; 4) activity in the EN components appears to be strongly caused by DMN (central EN is controlled by DMN2, visuo-motor coordination is controlled by DMN1, DMN2 [TPJ], and DMN3 [PCC], salience EN is controlled by DMN1, DMN2 [TPJ], and DMN3 [PCC]). These results together suggest that DMN components cause activity in EN components (Uddin et al. 2009) and reveal a key top-down role played by the PCC (Jiao et al. 2011). The very low frequency at which these causal relationships operate (see arrows color, all <0.1 Hz) reveals that they were not due to physiological noise (respiratory ranges from 0.1 to 0.5 Hz, cardiac from 0.6 to 1.2 Hz) but to actual functional interactions (Cordes et al. 2001).

General Linear Model Analysis

The previous ICA and Granger causality analyses served to characterize overall activity during the task. To characterize activation differences between congruent and incongruent trials, we used a GLM analysis. For the various statistical contrasts (random effects, all corrected for multiple comparisons with FDR, q(FDR) < 0.05), we used 7 different factors, consisting of the 6 prime/cue combinations (congruent, neutral, and incongruent for both ipsilateral and contralateral correct responses) and the errors trials (ipsilateral responses instead of contralateral ones or vice versa). Trials with no response were disregarded (only 2 trials for one subject).

Brain regions showing selective increases and decreases of activity during correct performance were identified by contrasting correct trials versus baseline. Consistently with the ICA analyses, several lateral frontal, parietal, and temporal regions associated with EN increased their activation during task performance (Supplementary Table S1), whereas a number of regions—more active during baseline and associated with the DMN—decreased their activity during task execution (Supplementary Table S2).

We also looked for selective activity during error trials, as compared with correct trials, and we found 3 main regions in the salience EN (insula and anterior cingulate cortex; Supplementary Table S3). It is noteworthy that regions in the DMN, normally deactivated during correct performance, were instead not deactivated during error trials if compared with baseline (i.e., no region survived in the contrast of higher activations during baseline compared with error trials) (Sonuga-Barke and Castellanos 2007).

Given that the behavioral data showed that a priming effect took place only during prime/cue incongruency, in the key contrast we looked for brain activity involved during incongruent versus neutral trials (Fig. 5). It is important to underline that in this crucial contrast, we were looking at unconscious interference in task-set preparation and, simultaneously, we were excluding perceptual interference. This is because prime and cue were visually different both in incongruent and neutral trials, but it is only in the incongruent trials that unconscious primes coded for (contradictory) instructions. A number of regions in DMN showed decreased

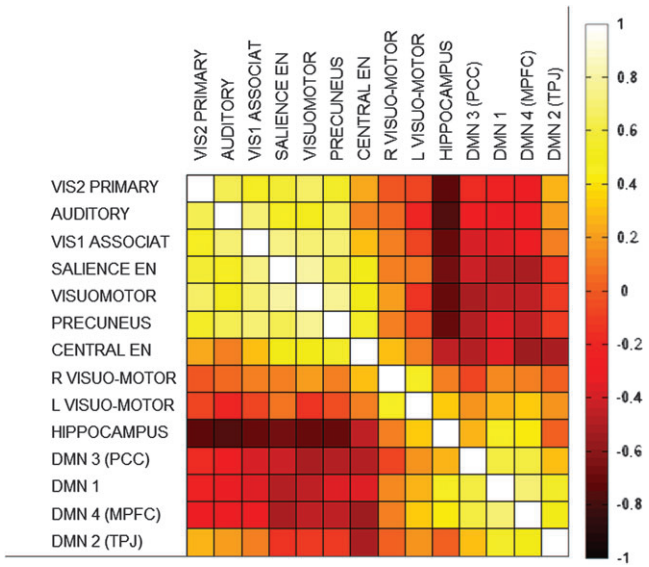

Figure 3. Average pairwise Pearson correlation values of time course activities of ICA components (after removal of artifacts) during task execution, grouped using a *k*-nearest neighbor algorithm. Brain activities split into 2 general anticorrelated groups, one including EN components and one including DMN components (see Table 1 for a list of the specific regions in each network).

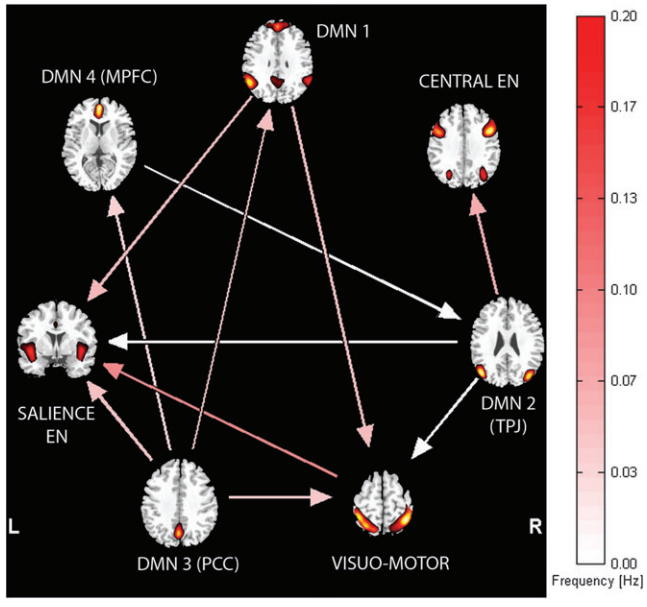

Figure 4. Granger Causality relationships (G-causality) for default and executive components from the ICA analysis. Arrows' color indicates frequency, arrows' width is proportional to the strength of the relationship, and their direction indicates a cause-effect relationship. We report only significant relationships (1 Samp. *T*-test significant, FDR corrected for multiple comparisons $q < 0.05$).

activity during this contrast, whereas a number of regions in EN showed increased activation (Table 2).

In another contrast, we looked at activity during neutral trials versus congruent trials, which showed only a right occipital region (Brodmann area 18, $x = 14$, $y = -77$, $z = 23$).

Finally, in a ROI analysis, we specifically looked at activity in the salience and central EN and in DMN1 and DMN4 (medial prefrontal) component (Fig. 6). The activity in the incongruent trials compared with the neutral and congruent cases increased in the EN and decreased in the DMN components both for ipsilateral and contralateral trials.

Summarizing, the GLM analysis confirmed that the group effects of incongruent trials during the task consisted of increased activation in EN and increased deactivation in the DMN.

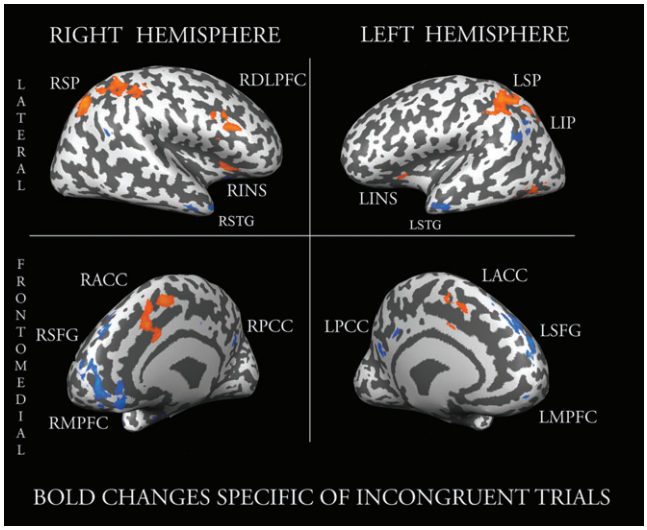

Figure 5. Activated (orange) and deactivated (blue) regions during incongruent trials relative to neutral trials. Acronyms: L and R at the beginning stand for left and right; SFG, superior frontal gyrus; MPFC, medial prefrontal; DLPFC, dorsolateral prefrontal; ACC, anterior cingulate; INS, insula; PCC, posterior cingulate; SP, superior parietal; IP, inferior parietal; STG, superior temporal gyrus.

Table 2

Brain regions identified with the contrast incongruent versus neutral trials (see Fig. 5)

Anatomical location	BA	*X*	*Y*	*Z*	*t*-value
Activation increases					
R. middle frontal gyrus (RDLPFC)	9	42	17	28	3.60
L. middle frontal gyrus (LDLPFC)	9	−39	20	26	3.37
R. insula (RINS)	13	33	20	4	3.91
L. insula (LINS)	13	−32	17	1	3.38
R. cingulate gyrus (RACC)	32	3	20	34	3.52
L. cingulate gyrus (LACC)	32	−3	19	36	3.27
R. superior parietal lobule (RSP)	7	24	−59	40	3.54
L. superior parietal lobule (LSP)	7	−25	−61	43	3.41
Activation decreases					
R. superior frontal gyrus (RSFG)	10	10	53	10	4.93
L. superior frontal gyrus (LSFG)	10	−16	56	27	4.49
R medial frontal gyrus (RMPFC)	10	7	37	−5	4.56
L medial frontal gyrus (LMPFC)	10	−6	49	−5	3.41
L. posterior cingulate (LPCC)	29	−12	−48	10	7.12
R. posterior cingulate (RPCC)	29	2	−50	29	4.59
R. supramarginal gyrus (RIP)	40	54	−48	22	3.97
L. supramarginal gyrus (LIP)	40	−50	−57	27	4.72
R superior temporal gyrus (RSTG)	21	40	9	−16	4.66
L. superior temporal gyrus (LSTG)	38	−52	2	−17	4.47

Note: Labels for foci of ROIs reported in the figure are in bold font. (q(FDR) < 0.05; cluster size threshold 150 mm^3). We report Talairach coordinates (*x*, *y*, *z*) (Talairach and Tournoux 1988) and the corresponding Brodmann's area label (BA).

Interindividual Brain–Behavior Relationship

We assessed if predictors could be derived from the DMN and EN for task performance. Based on previous studies, we looked at the relationship of anticorrelation strength and task performance at the single-subject level (Kelly et al. 2008). In this analysis, we expected to find that the anticorrelations between default and executive components would be stronger in subjects performing more efficiently, particularly in the more demanding incongruent conditions, where the unconscious primes conflicted with the conscious cues (Kelly et al. 2008). The individual anticorrelations between ENs and DMNs during the various conditions varied greatly (from between −0.6 and 0.4). We found significant effects on RT means in the various conditions only for the negative correlation of DMN1 and salience EN, such that interindividual speed during performance increased with increasing anticorrelation (Fig. 7). This effect reached significance only for the more demanding incongruent trials (those in which there is interference), for both ipsilateral and contralateral trials.

Discussion

In this behavioral and functional neuroimaging study, we investigated the effects of unconscious priming instruction on large-scale brain networks known to be modulated by task demands, namely ENs and DMNs. We found that unconscious primes interfered with performance when they were incongruent with the cues. This interference acted at the executive control level because a purely visual difference between a neutral prime and a cue did not produce behavioral effects (in RT or accuracy). The degree of control required to execute the responses (ipsilateral responses were less effortful than contralateral responses) did not affect unconscious priming. That is, the interference effect was obtained independently of whether the unconscious prime concerned the ipsilateral or the contralateral response. Using fMRI, with correlation and clustering analyses of the averaged Pearson's values, we individuated the independent anticorrelated networks involved during task execution, and with Granger causality analyses, we found that DMN components had a causal role on the activity in EN. GLM analyses revealed that the specific involvement of regions belonging to these networks (compared with activity during baseline) led to increased activations in ENs and decreased activations in DMNs. Investigation of the effects of the unconscious incongruent primes revealed decreased activations in DMN components and increased activations in EN components compared with the neutral trials. Finally, intersubject differences in speed during incongruent trials correlated with opposing effects between salience EN and a DMN component (DMN1).

Activity increases in executive regions have been reported in other studies (Lau and Passingham 2007; van Gaal et al. 2008, 2010). Our results confirm the emerging view that executive control is not necessarily tied to consciousness (Hommel 2007; Suhler and Churchland 2009), contrary to traditional research which identified it with intentional control and assumed that it necessarily requires consciousness (Jacoby 1991; Jack and Shallice 2001). Our results are also consistent with a recent study (Ursu et al. 2009) showing that anterior cingulate areas

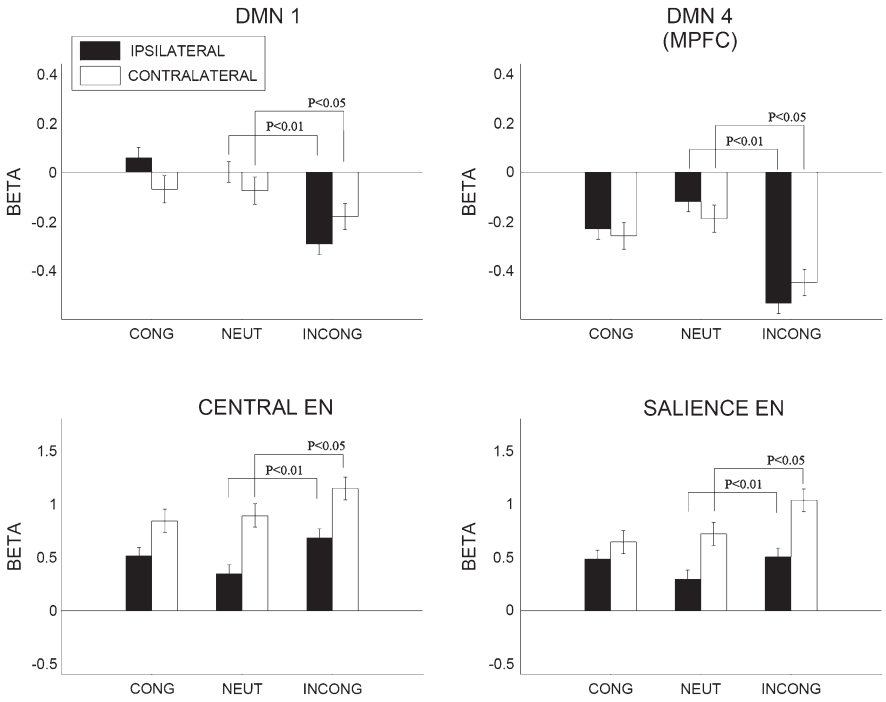

Figure 6. ROIs activities in the various prime/cue combinations. In these DMN components (DMN1 and DMN4), the amount of deactivations during incongruent trials is significantly stronger compared to activity during the neutral trials (for ipsilateral trials $P < 0.01$, for contralateral trials $P < 0.05$, *t*-test). In these EN components (central and salience), the increase of activation during incongruent trials is significantly higher than the activation during neutral trials (for ipsilateral trials $P < 0.01$, for contralateral trials $P < 0.05$, *t*-test). Error bars are standard errors.

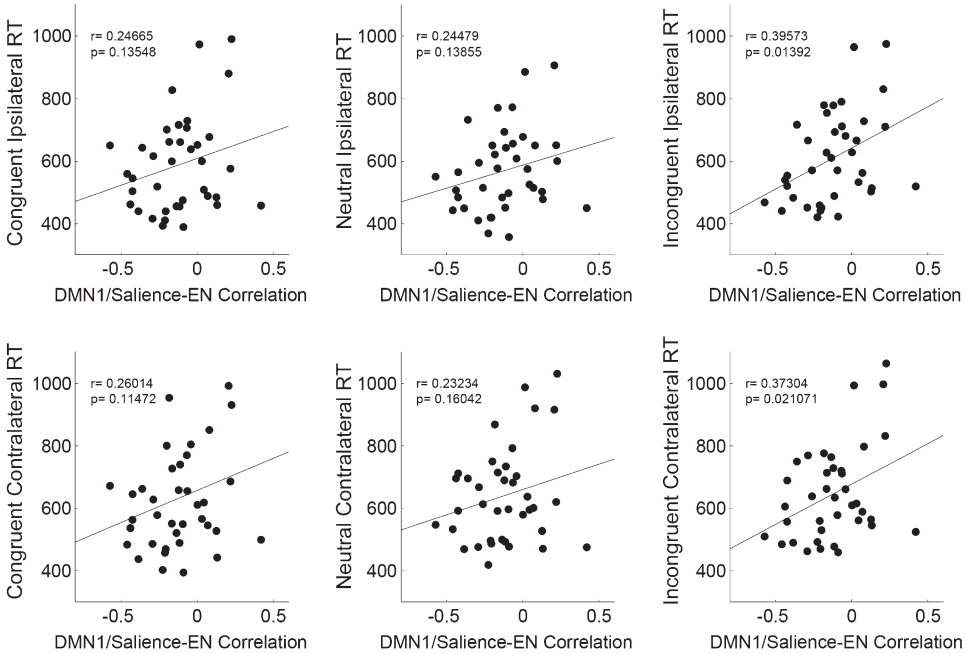

Figure 7. Distributions of single-subject's mean RTs (2 runs for each subject) during all 6 possible trial combinations (congruent/neutral/incongruent × ipsilateral/contralateral) as a function of the temporal correlation coefficient between DMN1 and salience EN. Faster RTs are consistent with stronger anticorrelations, but this is significant only for the most difficult condition, namely incongruent trials ($P < 0.05$), as in Kelly et al. (2008).

are sensitive to unconscious conflict created by an implicit probabilistic learning rule. In that study, volunteers had to respond to a stimulus location that changed according to rule they were not aware of, but that they had learned implicitly. Unbeknownst to the subjects, the stimulus location occasionally broke the implicit rule. An ROI analysis revealed that anterior cingulate cortex increased its activity for these trials presumably because they presented an unconscious conflict. This area is known to be more active in the presence of response conflict (Botvinick et al. 2004) at various time scales (De Pisapia and Braver 2006). However, Ursu et al. (2009) for the first time found that such conflict detection can act

unconsciously. In our experiment, we also found that anterior cingulate regions—almost overlapping with the regions in Ursu et al. (2009) (see Table 1)—were sensitive to the unconscious conflict generated by the incongruent primes. We have interpreted this effect in the context of activity in salience EN (its activity is reported in Fig. 7), of which anterior cingulate cortex is a part (Seeley et al. 2007). Further studies will have to investigate in detail how the anterior cingulate component interacts with the rest of the salience EN in both conscious and unconscious processing of information.

Our study extends previous findings by showing that unconscious conflicting primes not only increase activation in specific executive regions, but they concurrently deactivate DMN components. Using effective connectivity analyses, we revealed that the DMN plays a leading role throughout task execution. As already noted, the crucial role of DMN in task execution was recently emphasized in a study by Uddin et al. (2009). This convergence of results suggests that the DMN indirectly regulates task execution by decreasing activity in EN when there is no task to perform or when the task is not particularly demanding, and by deactivating itself when the external demands increase. Our findings additionally suggest that these dynamics can be modulated by unconscious demands. Along these lines, we find that a greater coordination between DMN components and salience EN was associated with faster and more efficient performance, thus suggesting that suppression of DMN activity during task execution is as important as EN increased activations.

Recent studies support the view that it is the salience EN (including insular and anterior cingulate cortex)—and not the central EN—that supports a basic domain independent and externally directed task mode anticorrelated to DMN (Braver and Barch 2006; Dosenbach et al. 2006, 2007). Our findings additionally show that its functional connectivity with DMN components predicts performance efficiency even in the case of unconscious, task-related information. Notably, with a whole-brain GLM analysis we found that salience regions were strongly activated during error trials (Supplementary Table S3), whereas regions in the DMN, normally deactivated during correct executions, were instead not deactivated if compared with baseline (i.e., no region survived in the contrast of higher activations during baseline compared with error trials). This suggests that during error trials there was low anticorrelation between salience ENs and DMNs. We did not investigate further this aspect because of the very low percentage of errors in this task (ranging on average between 3% and 6%).

While Granger analyses indicate significant causal relationships between DMN and EN, further examination of these claims is required to fully support the hypothesis that DMN regulates activity in EN (during both conscious and unconscious processing of information). Inferences about regional effective connectivity based on Granger causality analyses could be criticized on the grounds that it is possible that hemodynamic delays of BOLD signals might vary systematically between regions, independently of actual causal relationships. One response to this criticism is that studies of the BOLD signal have not found such regional systematicity in temporal variability (Miezin et al. 2000). Additionally, the Granger causality analyses in our study are based not on regional but on ICA components' time courses, a method that several other studies have shown to reliably individuate causal relationships between networks (Londei et al. 2007; Jafri et al. 2008; Demirci et al. 2009; Havlicek et al. 2010; Liao et al. 2010), and which has the additional advantage of not requiring the choice of seed regions, as done for regional Granger analyses.

What is the general functional significance of these unconscious DMN modulations driven by unconscious priming instructions? Soon et al. (2008) found that human "voluntary" motor decisions are coded in DMN regions and suggested that this network might control and determine upcoming decisions long before subjects are consciously aware of them. Our study additionally suggests that such unconscious future-oriented information processing taking place in DMN can be influenced by external masked instruction and primed without awareness. In general, the topic of how external stimuli affect DMN activity is currently highly debated (Gilbert et al. 2007; Northoff et al. 2010). One prominent interpretation is that DMN acts as a "sentinel" capable of monitoring the outside world but in an unfocussed and passive mode (Shulman et al. 1997; Gusnard and Raichle 2001; Gilbert et al. 2007; Hahn et al. 2007). Based on our results and in the light of other studies (Uddin et al. 2009) showing that DMN components have a causal role on EN, we support the view of a sentinel-like role for DMN and, additionally, propose that it might unconsciously monitor for the need of interrupting the stream of thoughts (McKiernan et al. 2006). In our study, the task was extremely simple and quickly routinized, but a demand for a higher external focus was triggered unconsciously by a masked contradictory instruction during incongruent trials, inducing uncertainty in the cognitive system about the specific course of actions to take. Such interference required a resolution in favor of the conscious goal, and thus, a deactivation in DMN allowed for a higher amount of focused attention compared with the case when there was no such conflict (the congruent and the neutral case). Such capacity for unconscious broad monitoring might be a necessity not just when the cognitive system is fully engaged in internal-oriented thinking (Buckner and Carroll 2007), but in particular when—in parallel—it is executing a very simple and routinized task, a situation known to engage a concurrent recruitment of default and executive regions (Christoff et al. 2009). In such situations, the subjective experience of mind wandering is accompanied by a task execution "in the background" (as happens, e.g., when a person is absorbed in her thoughts while driving on a well-known road). In such defocused situations, it would be inconvenient for the cognitive system to be completely detached from the environment, in case of an unexpected or salient task-related stimulus requiring increased attention (in the driving example, an unpredicted obstacle appearing in front of the vehicle or the exit signal). In such settings, a sentinel mechanism capable of an unconscious monitoring of the environment allows the individual to decouple from the internal processing and focus more on the external task when needed. A topic for future research will also be how unconscious monitoring in DMN relates to the observation that people who are mind wandering during simple task executions can either be aware of their drifting thoughts (tuning out) or be so immersed in their internal thoughts that they are not aware of them (zoning-out) (Smallwood et al. 2008).

The main purpose of our study was to investigate the effects of exogenous unconscious priming instructions on ENs and DMNs. We found that unconscious instructions conflicting with consciously visible instructions disengaged activities in

DMN and increased activity in EN. This study suggests that the involvement of DMN in unfocused and broad watchfulness (Shulman et al. 1997; Gusnard and Raichle 2001; Gilbert et al. 2007; Hahn et al. 2007) and in the allocation of attentional resources in EN (Raichle et al. 2001; Greicius et al. 2003; Fox, Corbetta, et al. 2006; Fransson 2006; Christoff et al. 2009) can also act in the absence of awareness.

Funding

Società Scienze Mente Cervello (SMC)/Fondazione Cassa di Risparmio di Trento e Rovereto; Provincia Autonoma di Trento (Italy) Project PAT Post-doc 2006 (to P. L.).

Supplementary Material

Supplementary material can be found at: http://www.cercor.oxfordjournals.org/

Notes

Conflict of Interest: None declared.

References

Andrews-Hanna JR, Reidler JS, Sepulcre J, Poulin R, Buckner RL. 2010. Functional-anatomic fractionation of the brain's default network. Neuron. 65:550–562.

Bell AJ, Sejnowski TJ. 1995. An information-maximization approach to blind separation and blind deconvolution. Neural Comput. 7:1129–1159.

Botvinick MM, Cohen JD, Carter CS. 2004. Conflict monitoring and anterior cingulate cortex: an update. Trends Cogn Sci. 8:539–546.

Brainard DH. 1997. The Psychophysics Toolbox. Spat Vis. 10:433–436.

Braver TS, Barch DM. 2006. Extracting core components of cognitive control. Trends Cogn Sci. 10:529–532.

Breitmeyer B, Öğmen H. 2006. Visual masking: time slices through conscious and unconscious vision. Oxford: Oxford University Press.

Breitmeyer BG. 2007. Visual masking: past accomplishments, present status, future developments. Adv Cogn Psychol. 3:9–20.

Bressler SL, Menon V. 2010. Large-scale brain networks in cognition: emerging methods and principles. Trends Cogn Sci. 14:277–290.

Buckner RL, Andrews-Hanna JR, Schacter DL. 2008. The brain's default network: anatomy, function, and relevance to disease. Ann N Y Acad Sci. 1124:1–38.

Buckner RL, Carroll DC. 2007. Self-projection and the brain. Trends Cogn Sci. 11:49–57.

Calhoun VD, Adali T, Pearlson GD, Pekar JJ. 2001. A method for making group inferences from functional MRI data using independent component analysis. Hum Brain Mapp. 14:140–151.

Calhoun VD, Kiehl KA, Pearlson GD. 2008. Modulation of temporally coherent brain networks estimated using ICA at rest and during cognitive tasks. Hum Brain Mapp. 29:828–838.

Christoff K, Gordon AM, Smallwood J, Smith R, Schooler JW. 2009. Experience sampling during fMRI reveals default network and executive system contributions to mind wandering. Proc Natl Acad Sci U S A. 106:8719–8724.

Christoff K, Ream JM, Gabrieli JD. 2004. Neural basis of spontaneous thought processes. Cortex. 40:623–630.

Cordes D, Haughton VM, Arfanakis K, Carew JD, Turski PA, Moritz CH, Quigley MA, Meyerand ME. 2001. Frequencies contributing to functional connectivity in the cerebral cortex in "resting-state" data. AJNR Am J Neuroradiol. 22:1326–1333.

Damoiseaux JS, Rombouts SA, Barkhof F, Scheltens P, Stam CJ, Smith SM, Beckmann CF. 2006. Consistent resting-state networks across healthy subjects. Proc Natl Acad Sci U S A. 103:13848–13853.

Dehaene S, Naccache L. 2001. Towards a cognitive neuroscience of consciousness: basic evidence and a workspace framework. Cognition. 79:1–37.

Del Cul A, Baillet S, Dehaene S. 2007. Brain dynamics underlying the nonlinear threshold for access to consciousness. PLoS Biol. 5:e260.

Demirci O, Stevens MC, Andreasen NC, Michael A, Liu J, White T, Pearlson GD, Clark VP, Calhoun VD. 2009. Investigation of relationships between fMRI brain networks in the spectral domain using ICA and Granger causality reveals distinct differences between schizophrenia patients and healthy controls. Neuroimage. 46:419–431.

De Pisapia N, Braver TS. 2006. A model of dual control mechanisms through anterior cingulate and prefrontal cortex interactions. Neurocomputing. 69:1322–1326.

Dosenbach NU, Fair DA, Miezin FM, Cohen AL, Wenger KK, Dosenbach RA, Fox MD, Snyder AZ, Vincent JL, Raichle ME, et al. 2007. Distinct brain networks for adaptive and stable task control in humans. Proc Natl Acad Sci U S A. 104:11073–11078.

Dosenbach NU, Visscher KM, Palmer ED, Miezin FM, Wenger KK, Kang HC, Burgund ED, Grimes AL, Schlaggar BL, Petersen SE. 2006. A core system for the implementation of task sets. Neuron. 50:799–812.

Esposito F, Bertolino A, Scarabino T, Latorre V, Blasi G, Popolizio T, Tedeschi G, Cirillo S, Goebel R, Di Salle F. 2006. Independent component model of the default-mode brain function: assessing the impact of active thinking. Brain Res Bull. 70:263–269.

Fox MD, Corbetta M, Snyder AZ, Vincent JL, Raichle ME. 2006. Spontaneous neuronal activity distinguishes human dorsal and ventral attention systems. Proc Natl Acad Sci U S A. 103:10046–10051.

Fox MD, Snyder AZ, Vincent JL, Corbetta M, Van Essen DC, Raichle ME. 2005. The human brain is intrinsically organized into dynamic, anticorrelated functional networks. Proc Natl Acad Sci U S A. 102:9673–9678.

Fox MD, Snyder AZ, Zacks JM, Raichle ME. 2006. Coherent spontaneous activity accounts for trial-to-trial variability in human evoked brain responses. Nat Neurosci. 9:23–25.

Fransson P. 2006. How default is the default mode of brain function? Further evidence from intrinsic BOLD signal fluctuations. Neuropsychologia. 44:2836–2845.

Genovese CR, Lazar NA, Nichols T. 2002. Thresholding of statistical maps in functional neuroimaging using the false discovery rate. Neuroimage. 15:870–878.

Gilbert SJ, Dumontheil I, Simons JS, Frith CD, Burgess PW. 2007. Comment on "Wandering minds: the default network and stimulus-independent thought". Science. 317:43.

Goebel R, Roebroeck A, Kim DS, Formisano E. 2003. Investigating directed cortical interactions in time-resolved fMRI data using vector autoregressive modeling and Granger causality mapping. Magn Reson Imaging. 21:1251–1261.

Golland Y, Bentin S, Gelbard H, Benjamini Y, Heller R, Nir Y, Hasson U, Malach R. 2007. Extrinsic and intrinsic systems in the posterior cortex of the human brain revealed during natural sensory stimulation. Cereb Cortex. 17:766–777.

Greicius MD, Kiviniemi V, Tervonen O, Vainionpaa V, Alahuhta S, Reiss AL, Menon V. 2008. Persistent default-mode network connectivity during light sedation. Hum Brain Mapp. 29:839–847.

Greicius MD, Krasnow B, Reiss AL, Menon V. 2003. Functional connectivity in the resting brain: a network analysis of the default mode hypothesis. Proc Natl Acad Sci U S A. 100:253–258.

Gusnard DA, Raichle ME. 2001. Searching for a baseline: functional imaging and the resting human brain. Nat Rev Neurosci. 2:685–694.

Haggard P. 2008. Human volition: towards a neuroscience of will. Nat Rev Neurosci. 9:934–946.

Hahn B, Ross TJ, Stein EA. 2007. Cingulate activation increases dynamically with response speed under stimulus unpredictability. Cereb Cortex. 17:1664–1671.

Havlicek M, Jan J, Brazdil M, Calhoun VD. 2010. Dynamic Granger causality based on Kalman filter for evaluation of functional network connectivity in fMRI data. Neuroimage. 53:65–77.

Hommel B. 2007. Consciousness and control—not identical twins. J Consciousness Stud. 14:155–176.

Jack AI, Shallice T. 2001. Introspective physicalism as an approach to the science of consciousness. Cognition. 79:161–196.

Jacoby LL. 1991. A process dissociation framework—separating automatic from intentional uses of memory. J Mem Lang. 30:513–541.
Jafri MJ, Pearlson GD, Stevens M, Calhoun VD. 2008. A method for functional network connectivity among spatially independent resting-state components in schizophrenia. Neuroimage. 39:1666–1681.
Jiao Q, Lu G, Zhang Z, Zhong Y, Wang Z, Guo Y, Li K, Ding M, Liu Y. 2011. Granger causal influence predicts BOLD activity levels in the default mode network. Hum Brain Mapp. 32:154–161.
Kane MJ, Engle RW. 2003. Working-memory capacity and the control of attention: the contributions of goal neglect, response competition, and task set to Stroop interference. J Exp Psychol Gen. 132:47–70.
Kelly AM, Uddin LQ, Biswal BB, Castellanos FX, Milham MP. 2008. Competition between functional brain networks mediates behavioral variability. Neuroimage. 39:527–537.
Kelly RE, Jr, Alexopoulos GS, Wang Z, Gunning FM, Murphy CF, Morimoto SS, Kanellopoulos D, Jia Z, Lim KO, Hoptman MJ. 2010. Visual inspection of independent components: defining a procedure for artifact removal from fMRI data. J Neurosci Methods. 189:233–245.
Kim H. 2010. Dissociating the roles of the default-mode, dorsal, and ventral networks in episodic memory retrieval. Neuroimage. 50:1648–1657.
Kouider S, Dehaene S. 2007. Levels of processing during non-conscious perception: a critical review of visual masking. Philos Trans R Soc Lond B Biol Sci. 362:857–875.
Larson-Prior LJ, Zempel JM, Nolan TS, Prior FW, Snyder AZ, Raichle ME. 2009. Cortical network functional connectivity in the descent to sleep. Proc Natl Acad Sci U S A. 106:4489–4494.
Lau HC, Passingham RE. 2007. Unconscious activation of the cognitive control system in the human prefrontal cortex. J Neurosci. 27:5805–5811.
Leonard CJ, Chiu YC. 2007. What you set is not what you see: unconscious activation of cognitive control. J Neurosci. 27:11170–11171; discussion: 11170.
Liao W, Mantini D, Zhang Z, Pan Z, Ding J, Gong Q, Yang Y, Chen H. 2010. Evaluating the effective connectivity of resting state networks using conditional Granger causality. Biol Cybern. 102:57–69.
Lin P, Hasson U, Jovicich J, Robinson S. 2011. A neuronal basis for task-negative responses in the human brain. Cereb Cortex. 21:821–830.
Londei A, D'Ausilio A, Basso D, Sestieri C, Del Gratta C, Romani GL, Belardinelli MO. 2007. Brain network for passive word listening as evaluated with ICA and Granger causality. Brain Res Bull. 72:284–292.
Macmillan N, Creelman C. 1991. Detection theory: a user's guide. New York: Cambridge University Press.
Martuzzi R, Ramani R, Qiu M, Rajeevan N, Constable RT. 2010. Functional connectivity and alterations in baseline brain state in humans. Neuroimage. 49:823–834.
McKiernan KA, D'Angelo BR, Kaufman JN, Binder JR. 2006. Interrupting the "stream of consciousness": an fMRI investigation. Neuroimage. 29:1185–1191.
McVay JC, Kane MJ. 2010. Does mind wandering reflect executive function or executive failure? Comment on Smallwood and Schooler (2006) and Watkins (2008). Psychol Bull. 136:188–197discussion 198–207.
Mennes M, Kelly C, Zuo XN, Di Martino A, Biswal BB, Castellanos FX, Milham MP. 2010. Inter-individual differences in resting-state functional connectivity predict task-induced BOLD activity. Neuroimage. 50:1690–1701.
Mennes M, Zuo XN, Kelly C, Di Martino A, Zang YF, Biswal B, Castellanos FX, Milham MP. 2011. Linking inter-individual differences in neural activation and behavior to intrinsic brain dynamics. Neuroimage. 54(4):2950–2959.
Miezin FM, Maccotta L, Ollinger JM, Petersen SE, Buckner RL. 2000. Characterizing the hemodynamic response: effects of presentation rate, sampling procedure, and the possibility of ordering brain activity based on relative timing. Neuroimage. 11:735–759.
Northoff G, Qin P, Nakao T. 2010. Rest–stimulus interaction in the brain: a review. Trends Neurosci. 33:277–284.
Proctor RW, Reeve TG. 1990. Research on stimulusresponse compatibility: toward a comprehensive account. In: Proctor RW, editor. Stimulusresponse compatibility: an integrated perspective. Amsterdam (North-Holland). p. 483–494.
Raichle ME, MacLeod AM, Snyder AZ, Powers WJ, Gusnard DA, Shulman GL. 2001. A default mode of brain function. Proc Natl Acad Sci U S A. 98:676–682.
Rees G, Kreiman G, Koch C. 2002. Neural correlates of consciousness in humans. Nat Rev Neurosci. 3:261–270.
Roebroeck A, Formisano E, Goebel R. 2005. Mapping directed influence over the brain using Granger causality and fMRI. Neuroimage. 25:230–242.
Seeley WW, Menon V, Schatzberg AF, Keller J, Glover GH, Kenna H, Reiss AL, Greicius MD. 2007. Dissociable intrinsic connectivity networks for salience processing and executive control. J Neurosci. 27:2349–2356.
Sergent C, Baillet S, Dehaene S. 2005. Timing of the brain events underlying access to consciousness during the attentional blink. Nat Neurosci. 8:1391–1400.
Seth AK. 2005. Causal connectivity of evolved neural networks during behavior. Network. 16:35–54.
Shulman GL, Fiez JA, Corbetta M, Buckner RL, Miezin FM, Raichle ME, Petersen SE. 1997. Common blood flow changes across visual tasks. 2. Decreases in cerebral cortex. J Cognitive Neurosci. 9:648–663.
Smallwood J, Beach E, Schooler JW, Handy TC. 2008. Going AWOL in the brain: mind wandering reduces cortical analysis of external events. J Cogn Neurosci. 20:458–469.
Smallwood J, Schooler JW. 2006. The restless mind. Psychol Bull. 132:946–958.
Sonuga-Barke EJ, Castellanos FX. 2007. Spontaneous attentional fluctuations in impaired states and pathological conditions: a neurobiological hypothesis. Neurosci Biobehav Rev. 31:977–986.
Soon CS, Brass M, Heinze HJ, Haynes JD. 2008. Unconscious determinants of free decisions in the human brain. Nat Neurosci. 11:543–545.
Sridharan D, Levitin DJ, Menon V. 2008. A critical role for the right fronto-insular cortex in switching between central-executive and default-mode networks. Proc Natl Acad Sci U S A. 105:12569–12574.
Suhler CL, Churchland PS. 2009. Control: conscious and otherwise. Trends Cogn Sci. 13:341–347.
Talairach J, Tournoux P. 1988. Co-planar stereotaxic atlas of the human brain. New York: Thieme.
Uddin LQ, Kelly AM, Biswal BB, Xavier Castellanos F, Milham MP. 2009. Functional connectivity of default mode network components: correlation, anticorrelation, and causality. Hum Brain Mapp. 30:625–637.
Ursu S, Clark KA, Aizenstein HJ, Stenger VA, Carter CS. 2009. Conflict-related activity in the caudal anterior cingulate cortex in the absence of awareness. Biol Psychol. 80:279–286.
van Gaal S, Ridderinkhof KR, Fahrenfort JJ, Scholte HS, Lamme VA. 2008. Frontal cortex mediates unconsciously triggered inhibitory control. J Neurosci. 28:8053–8062.
van Gaal S, Ridderinkhof KR, Scholte HS, Lamme VA. 2010. Unconscious activation of the prefrontal no-go network. J Neurosci. 30:4143–4150.
Vincent JL, Patel GH, Fox MD, Snyder AZ, Baker JT, Van Essen DC, Zempel JM, Snyder LH, Corbetta M, Raichle ME. 2007. Intrinsic functional architecture in the anaesthetized monkey brain. Nature. 447:83–86.
Weissman DH, Roberts KC, Visscher KM, Woldorff MG. 2006. The neural bases of momentary lapses in attention. Nat Neurosci. 9:971–978.
West R, Baylis GC. 1998. Effects of increased response dominance and contextual disintegration on the Stroop interference effect in older adults. Psychol Aging. 13:206–217.
Yang J, Weng X, Zang Y, Xu M, Xu X. 2010. Sustained activity within the default mode network during an implicit memory task. Cortex. 46:354–366.
Zaitsev M, Hennig J, Speck O. 2004. Point spread function mapping with parallel imaging techniques and high acceleration factors: fast, robust, and flexible method for echo-planar imaging distortion correction. Magn Reson Med. 52:1156–1166.